

## Supporting Information

### Composition Tunability and (111)-Dominant Facets of Ultrathin Platinum-Gold Alloy Nanowires toward Enhanced Electrocatalysis

Fangfang Chang<sup>1,2</sup>, Shiyao Shan<sup>1</sup>, Valeri Petkov<sup>3</sup>, Zakiya Skeete<sup>1</sup>, Aolin Lu<sup>1</sup>, Jonathan Ravid<sup>1</sup>, Jinfang Wu<sup>1</sup>, Jin Luo<sup>1</sup>, Gang Yu<sup>2</sup>, Yang Ren<sup>4</sup> and Chuan-Jian Zhong<sup>1,\*</sup>

<sup>1</sup> Department of Chemistry, State University of New York at Binghamton, Binghamton, New York 13902, USA.

<sup>2</sup> College of Chemistry and Chemical Engineering, Hunan University, Changsha 410082, China.

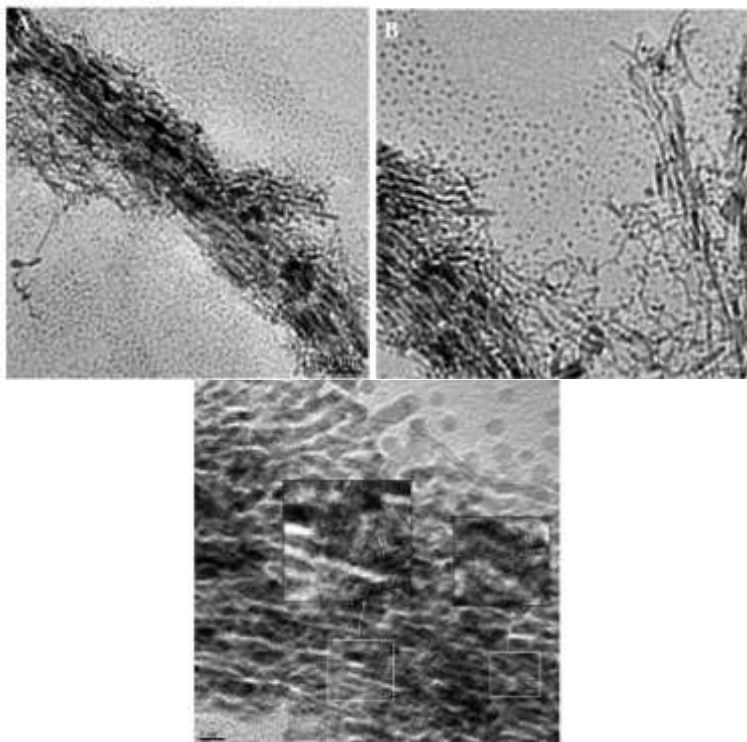
<sup>3</sup> Department of Physics, Central Michigan University, Mt. Pleasant, Michigan 48859, USA.

<sup>4</sup> X-ray Science Division, Advanced Photon Source, Argonne National Laboratory, Argonne, Illinois 60439, USA

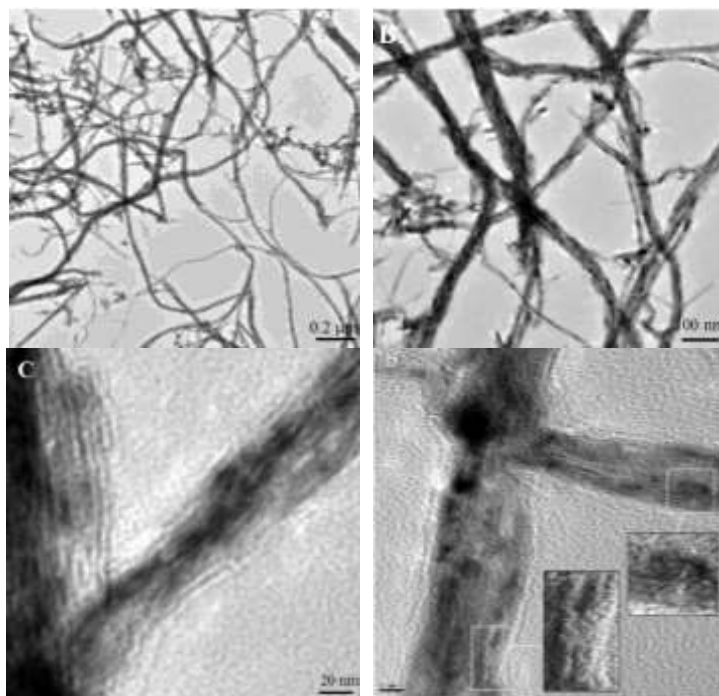
**Abstract.** The Supporting Information includes the additional experimental data: Table of chemical compositions of NWs, TEM and HR-TEM images for PtAu NWs of different compositions (Pt<sub>12</sub>Au<sub>88</sub>, Pt<sub>45</sub>Au<sub>55</sub> and Pt<sub>88</sub>Au<sub>12</sub>). TEM image for Pt<sub>76</sub>Au<sub>24</sub> NPs, XRD patterns for PtAu NWs/C catalysts with different bimetallic composition, XRD patterns for Pt<sub>76</sub>Au<sub>24</sub> NWs and NPs, CV curves, ECA, MA and SA data for NWs in comparison with data of Pt/C, Durability test for Pt<sub>76</sub>Au<sub>24</sub> NWs/C catalyst, Illustration of surface sites for a cubo-octahedral Pt<sub>151</sub>Au<sub>50</sub> cluster model, Calculated structure, binding energy and d-band center for PtAu clusters, calculated structure, adsorption energy and d-band center for molecularly adsorbed oxygen on PtAu clusters, adsorption energies of O<sub>2</sub> and intermediate O<sub>ads</sub> species on PtAu clusters,

**Table S1.** Chemical compositions of as-synthesized Pt<sub>n</sub>Au<sub>100-n</sub> NWs and Pt<sub>n</sub>Au<sub>100-n</sub> NWs supported on carbon.

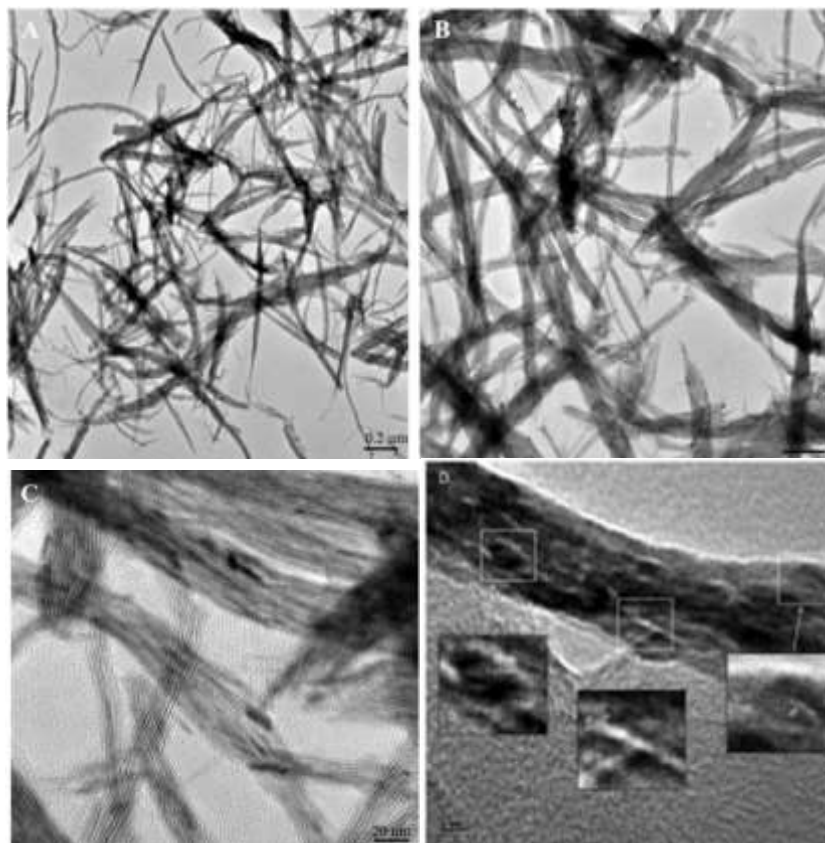
PtAu feeding ratio	As synthesized NWs	NWs on carbon
10:90	12:88	16:84
40:60	45:55	49:51
70:30	72:28	76:24
85:15	88:12	90:10



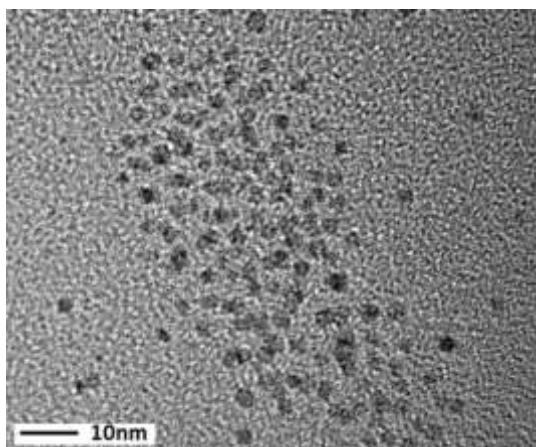
**Figure S1.** TEM and HR-TEM images for a sample of as-synthesized  $\text{Pt}_{12}\text{Au}_{88}$  nanowires with different magnifications. The average diameter of individual nanowires in the bundles is  $3.3 \pm 1.0$  nm. In C: the lattice fringes feature (111) facets with 0.234 nm.



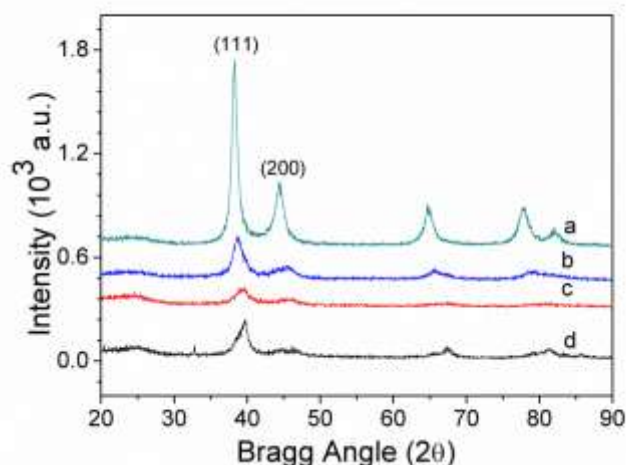
**Figure S2.** TEM and HR-TEM images for a sample of as-synthesized  $\text{Pt}_{45}\text{Au}_{55}$  nanowires with different magnifications. The average diameter of individual nanowires in the bundles is  $5.2 \pm 1.0$  nm. In D: the lattice fringes feature (111) facets with 0.233 nm.



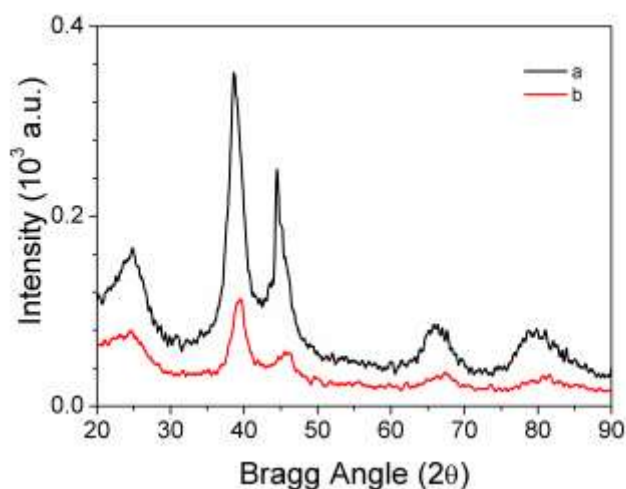
**Figure S3.** TEM and HR-TEM images for a sample of as-synthesized  $\text{Pt}_{88}\text{Au}_{12}$  nanowires with different magnifications. The average diameter of individual nanowires in the bundles is  $5.0 \pm 1.0$  nm. In D: the lattice fringes feature (111) facets with 0.231 nm.



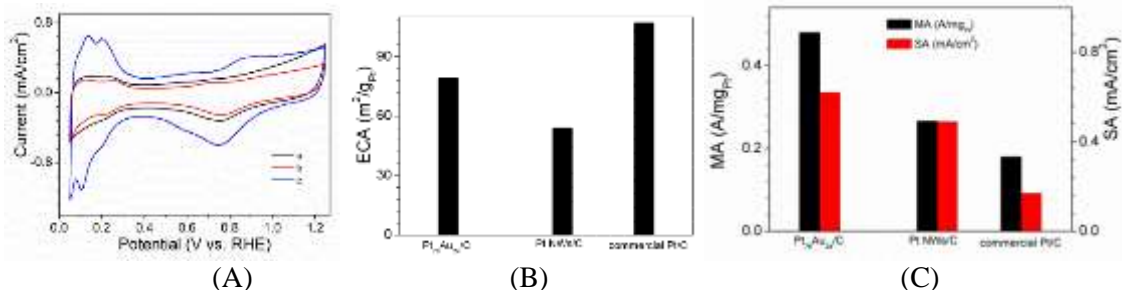
**Figure S4.** TEM image for  $\text{Pt}_{76}\text{Au}_{24}$  nanoparticles (size:  $3.0 \pm 1.0$  nm). The nanoparticle is as-synthesized, not supported on carbon and not thermally treated.



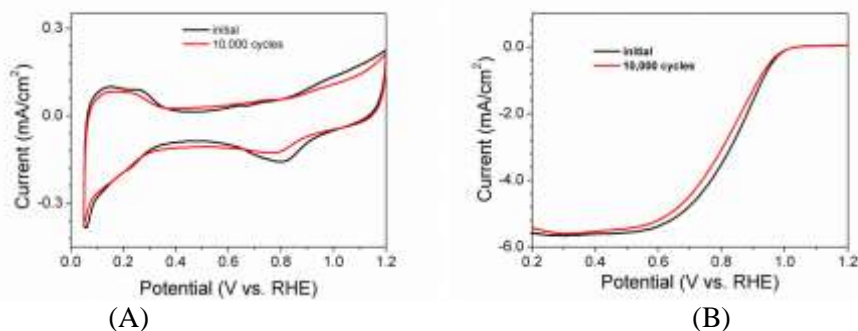
**Figure S5.** XRD patterns for PtAu NWs/C catalysts with different bimetallic composition: Pt<sub>16</sub>Au<sub>84</sub>/C (a), Pt<sub>49</sub>Au<sub>51</sub>/C (b), Pt<sub>76</sub>Au<sub>24</sub>/C (c), Pt<sub>90</sub>Au<sub>10</sub>/C (d). The chemical composition was determined by ICP-OES. The weak Bragg peak-like feature at  $2\theta$  of about  $24.5^\circ$  seen in the XRD patterns of all NWs is from the carbon support. Bragg peaks in the XRD patterns are broad but not split into two components indicating that PtAu NWs/C are single nanophase and segregated into Pt and Au nanophases. The conclusion is supported by the fact that peaks in the XRD patterns for PtAu NWs/C are positioned between those characteristic for pure Au and Pt metals.



**Figure S6.** XRD patterns of Pt<sub>76</sub>Au<sub>24</sub> NWs and NPs: (a) Pt<sub>76</sub>Au<sub>24</sub> NPs/C and (b) Pt<sub>76</sub>Au<sub>24</sub> NWs/C. Peaks in the XRD pattern of NWs are much sharper than those in the XRD pattern of NPs. The observation confirms the polycrystalline nature of Pt<sub>76</sub>Au<sub>24</sub> NWs. Note, the relative ratio between the intensities of (111) and (200) Bragg peaks in the XRD pattern of Pt<sub>76</sub>Au<sub>24</sub> NWs is higher as compared to the case of Pt<sub>76</sub>Au<sub>24</sub> NPs. The observation provides a clue as to why the electrocatalytic activity of NWs is higher than that of NPs.



**Figure S7.** (A) CV curves for Pt<sub>76</sub>Au<sub>24</sub> NWs/C (a, black), Pt NWs/C (b, red) and commercial Pt/C (c, blue). Electrode: Glassy carbon (0.196 cm<sup>2</sup>) inked with 10 μg catalysts; Electrolyte: 0.1 M HClO<sub>4</sub> saturated with N<sub>2</sub> (scan rate: 50 mV/s). (B) ECA values vs. Pt%. (C) Comparison of the MA and SA data at 0.900 V (vs. RHE) as a function of Pt% for Pt<sub>76</sub>Au<sub>24</sub> NWs/C, Pt NWs/C and commercial Pt/C.





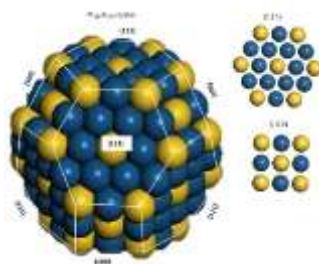



**Figure S8.** Durability test of Pt<sub>76</sub>Au<sub>24</sub> NWs/C catalyst for ORR. (A) CV curves at the beginning of potential cycling and at the end of 10,000 cycles (potential sweep rate, 50mV/s, potential cycle window: 0.6 and 1.1 V) in 0.1 M HClO<sub>4</sub> solution saturated with nitrogen. (B) RDE curve for ORR at the beginning of potential cycling and at the end of 10,000 cycles (scan rate: 10 mV/s and rotation speed: 1600 rpm).







**Figure S9.** The surface sites for a cubo-octahedral Pt<sub>151</sub>Au<sub>50</sub> cluster model (1.8 nm cluster size) with eight (111) and six (100) planes

**Table S2.** Structure, binding energy ( $E_{\text{binding}}$ ) and d-band center for  $\text{Pt}_n\text{Au}_{4-n}$  clusters.

	Cluster	$E_{\text{binding}}$ (eV)	d-band center (eV)
Pt <sub>4</sub>		1.02	-1.13
Pt <sub>3</sub> Au <sub>1</sub>		1.13	-1.16
Pt <sub>2</sub> Au <sub>2</sub>		1.19	-1.17
Pt <sub>1</sub> Au <sub>3</sub>		1.05	-1.19
Au <sub>4</sub>		1.05	-1.2

**Table S3.** Structure, adsorption energy ( $E_{\text{ads}}$ ) and d-band center for molecularly adsorbed  $\text{O}_2$  on  $\text{Pt}_n\text{Au}_{4-n}$  clusters

	Cluster	$E_{\text{ads}}$ (eV)	d-band center (eV)
Pt <sub>4</sub> -O <sub>2</sub>		1.46	-1.11
Pt <sub>3</sub> Au <sub>1</sub> -O <sub>2</sub>		1.56	-1.14
Pt <sub>2</sub> Au <sub>2</sub> -O <sub>2</sub>		1.50	-1.15
Pt <sub>1</sub> Au <sub>3</sub> -O <sub>2</sub>		1.51	-1.17

**Table S4.** Adsorption energies of  $\text{O}_2$  and intermediate  $\text{O}_{\text{ads}}$  on  $\text{Pt}_n\text{Au}_{4-n}$  clusters

Adsorption energy(eV)	$\text{Pt}_4$	$\text{Pt}_3\text{Au}_1$	$\text{Pt}_2\text{Au}_2$	$\text{Pt}_1\text{Au}_3$
$E_{\text{O}_2}$	1.46	1.56	1.50	1.51
$E_{\text{O}}$	4.93	4.69	4.72	4.74